Operating Point Selection in Multimodel Controller Design

Wen Tan, Horacio J. Marquez, and Tongwen Chen

***Abstract*— Gap metric for selecting operating points in multimodel controller design is discussed and extended to accommodate the performance requirement. It is shown that the loop-shaping $\mathcal{H}_\infty$ approach can integrate the procedure of selecting operating points and the local controller design. The local controllers can guarantee not only stability but also performance specified by the pre- and/or post-compensators. Thus at each operating points, local controllers can have similar performance, and the global performance of the system can be predicted.**

I. Introduction

Multimodel approach is a popular method for nonlinear control system design. The method represents the nonlinear system as a combination of linear systems. Local controllers can be designed using well-known linear design techniques, such as LQG, $\mathcal{H}_\infty$, etc.. The concept is simple, yet it is quite successful in practical controller design, see, for example, [1]–[3]. However, the question of how many models are sufficient in design and where the models should be selected is still unsolved.

Recently, Galan et. al. [4] suggested using gap metric as a guideline for selecting local models. The idea is that the 'distance' of two selected models should not be larger than a prescribed level. Since local controller can be designed to robustly stabilize all the models within the prescribed level, models selected in this way can guarantee the global stability of the closed-loop systems as long as the change of models is 'slow'. The method is practical in that a detailed nonlinear system model is not needed. However, stability is not the only requirement of a control system. Performance such as disturbance rejection, dynamic response etc. was not considered in the paper.

McNichols and Fadali [5] proposed to use interval mathematics and a classical synthesis design approach to determine a near minimal set of the design points. The algorithm made use of the closed-loop poles, since the performance of the closed-loop system is dependent on them. However, the approach is restricted to systems with 'interval' transfer functions, i.e., whose coefficients are within known intervals and vary slowly as a function of some external scheduling variable.

The measure of nonlinearity [6], [7] provides another viewpoint on selecting operating points for multimodel controller design. The idea is that we should select operating points near which the system is most 'nonlinear', so the local linear models can 'cover' the nonlinearity of the system. For the regime where the system is not so nonlinear, one linear model is sufficient. Unfortunately, the nonlinearity measure is usually not easy to compute, and a detailed nonlinear model is assumed to be available, which is often not possible to get in practice.

In this paper, we will extend the method in [4] to accommodate the performance requirement. Motivated by the loop-shaping $\mathcal{H}_\infty$ approach [8], we will use the gap metric for 'compensated' models as a guide for selecting operating points. With loop-shaping $\mathcal{H}_\infty$ design, the local controllers can guarantee not only stability but also performance specified by the pre- and/or post-compensators. Thus at each operating points, local controllers can have similar performance, and the global performance of the system can be predicted.

II. Gap Metric

In this section, we will review the theory of the gap metric. Details can be referred to [9]–[11].

The gap between two linear systems P_1 and P_2 is defined by

$$\delta(P_1,P_2) := \left\|\Pi_{\mathcal{G}(P_1)} - \Pi_{\mathcal{G}(P_2)}\right\|, \tag{1}$$

where $\mathcal{G}(\cdot)$ represents the graph of a linear operator, and Π denotes the orthogonal projection. Let $P_1 = N_1M_1^{-1}, P_2 = N_2M_2^{-1}$ be the normalized right coprime factorizations of P_1 and P_2, respectively, then

$$\mathcal{G}(P_1) = \begin{bmatrix} M_1 \\ N_1 \end{bmatrix}\mathcal{H}_2,\ \mathcal{G}(P_2) = \begin{bmatrix} M_2 \\ N_2 \end{bmatrix}\mathcal{H}_2. \tag{2}$$

The following result is well known:

Proposition 1 [10]

$$\delta(P_1,P_2) = \max\{\vec{\delta}(P_1,P_2), \vec{\delta}(P_2,P_1)\}, \tag{3}$$

where $\vec{\delta}(P_1,P_2)$ is the directed gap and can be computed by

$$\vec{\delta}(P_1,P_2) = \inf_{Q\in\mathcal{H}_\infty}\left\|\begin{bmatrix} M_1 \\ N_1 \end{bmatrix} - \begin{bmatrix} M_2 \\ N_2 \end{bmatrix} Q\right\|_\infty. \tag{4}$$

The gap metric is closely related to the coprime factor uncertainty description. We have

Proposition 2 [10] *Let P be a system with a normalized right coprime factorization $P = NM^{-1}$. Then for all $0 < \gamma \leq 1$,*

$$\begin{aligned}\{P_1 : \vec{\delta}(P,P_1) < \gamma\} \quad = \quad & \Big\{P_1 : P_1 = (N+\Delta_N)(M+\Delta_M)^{-1}, \\ & \Delta_N,\Delta_M \in \mathcal{H}_\infty, \left\|\begin{bmatrix} \Delta_N \\ \Delta_M \end{bmatrix}\right\|_\infty < \gamma\Big\}\end{aligned} \tag{5}$$

This work is partially sponsored by the Specialized Research Fund for the Doctoral Program of Higher Education (20020079007)

W. Tan is with the department of Automation, North China Electric Power University, Zhuxinzhuang, Dewai, Beijing, 102206, P. R. China, wtan@ieee.org

H. J. Marquez and T. Chen are with the department of Electrical & Computer Engineering, University of Alberta, Edmonton, AB T6G 2V4, Canada, marquez@ece.ualberta.ca, tchen@ece.ualberta.ca

The gap metric is thus very useful to characterize the robustness of a feedback system. Let P be a linear system and K be a stabilizing controller of P, denotes

$$b_{P,K} := \left\| \begin{bmatrix} I \\ K \end{bmatrix} (I+PK)^{-1} \begin{bmatrix} I & P \end{bmatrix} \right\|_\infty^{-1}, \qquad (6)$$

then we have

Proposition 3 [10] *Suppose the feedback system with the pair (P,K) is stable. Let*

$$\mathcal{P} := \{P_\Delta : \delta(P,P_\Delta) < \gamma_P\},\ \mathcal{K} := \{K_\Delta : \delta(K,K_\Delta) < \gamma_K\}. \quad (7)$$

Then the feedback system with the pair (P_Δ,K_Δ) is stable for all $P_\Delta \in \mathcal{P}$ and $K_\Delta \in \mathcal{K}$ if and only if

$$\arcsin(b_{P,K}) \geq \arcsin(\gamma_P) + \arcsin(\gamma_K). \qquad (8)$$

If there is no uncertainty in the controller K, i.e., $\gamma_K = 0$, then the feedback system with the pair (P_Δ,K) is stable for all $P_\Delta \in \mathcal{P}$ if and only if

$$\gamma_P \leq b_{P,K}. \qquad (9)$$

The result provides the theoretical background in applying the gap metric in selecting operating points for multimodel controller design. Suppose a certain operating point has been selected. The local model is P and the local controller is K. Then the next operating point should be selected at a distance (in the gap metric sense) no larger than $b_{P,K}$, since all models with a gap metric less than $b_{P,K}$ to the given model can be stabilized by the local controller K. To have a minimal set of the operating points, the next operating point should be selected at a distance exactly equal to $b_{P,K}$, or just a little smaller than it.

In practice, the local controller is not available before selecting the operating points, so we can first prescribe a distance level, and then starting from an initial operating point, compute the next operating point till the whole range of the operating points are covered.

III. Gap Metric for Shaped Plants

There are two drawbacks when applying the gap metric in selecting the operating points for multimodel controller design:

1) The gap metric is only related to robust stability, that is, the local controller K can only guarantee that it can stabilize the models at operating points close to the given operating point. However, stability is not the only issue in control system design. Other performance should also be guaranteed in selecting operating points.
2) In multimodel controller design, $b_{P,K}$ should be checked to make sure it is larger than the prescribed distance level, otherwise robust stability cannot be guaranteed.

Motivated by the loop shaping $\mathcal{H}_\infty$ approach [8], we propose to include performance weights in the gap metric computation.

Given a plant P, the loop shaping $\mathcal{H}_\infty$ design procedure goes as follows:

1) **Loop Shaping**. Pre-compensator W_1 and/or post-compensator W_2 are used to shape the singular values of P such that the shaped plant $\tilde{P} = W_2 P W_1$ has the desired open-loop shape.
2) **Robust Stabilization**. For the shaped plant $\tilde{P}$, find a controller $\tilde{K}$ such that the robust stability margin b_{opt} is maximized.

$$b_{\text{opt}}^{-1} = \inf_{\tilde{K}} \left\| \begin{bmatrix} I \\ \tilde{K} \end{bmatrix} (I+\tilde{P}\tilde{K})^{-1} \tilde{M}^{-1} \right\|_\infty \qquad (10)$$

   where $\tilde{P} = \tilde{M}^{-1}\tilde{N}$ is a left coprime factorization of $\tilde{P}$.
3) The final feedback controller is

$$K = W_1 \tilde{K} W_2 \qquad (11)$$

Clearly the method takes the performance into account by utilizing the pre- and/or post-compensators. It also solves a robust stabilization problem for the shaped plant, which guarantees that the performance of the shaped plants does not degrade even if there is uncertainty in the plant. If the coprime factorization is normalized, i.e.,

$$\tilde{M}\tilde{M}^{\sim} + \tilde{N}\tilde{N}^{\sim} = I \qquad (12)$$

it is easy to show that

$$b_{\text{opt}}^{-1} = \inf_{\tilde{K}} \left\| \begin{bmatrix} I \\ \tilde{K} \end{bmatrix} (I+\tilde{P}\tilde{K})^{-1} \begin{bmatrix} I & \tilde{P} \end{bmatrix} \right\|_\infty \qquad (13)$$

or

$$b_{\text{opt}} = \max_{\tilde{K}} b_{\tilde{P},\tilde{K}} \qquad (14)$$

So b_{opt} is the maximum of the robustness margin for the shaped plant $\tilde{P}$. Eq.(10) indicates that we can directly obtain b_{opt} with loop shaping $\mathcal{H}_\infty$ design.

The gap metric between the shaped plants thus has potential applications in selecting operating points for multimodel controller design. We compute the distance between the shaped models instead of the original models. Then a shaped model with a distance less than b_{opt} to a given (shaped) model at one operating point can be stabilized with the local optimal controller and the performance can be guaranteed.

IV. Compensator Selection and Multimodel Controller Design

We need to choose the pre- and/or post-compensators to reflect the performance requirements. How should we choose the compensators? Or in other word, what are the desired open-loop shapes?

The desired open-loop shape normally means high gain at low frequencies, roll-off rates of approximately 20 dB/decade at the desired bandwidth(s), and higher rates at high frequencies [11]. It is illustrated in Fig. 1.

To obtain a desired loop shape, we can choose the pre- and post-compensators following the guidelines [12]:

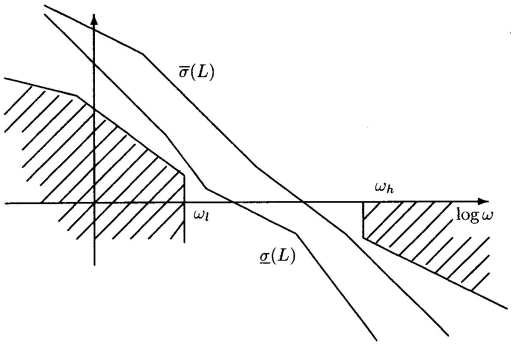

Fig. 1. The desired open-loop shape

1) The post-compensator W_2 is usually chosen as a constant, reflecting the relative importance of the outputs to be controlled. It is often set to an identity matrix if the model is well scaled.
2) In general the pre-compensator W_1 has the form $W_1 = W_p W_a W_g$.
   - W_p contains dynamic shaping. Integral action for low frequency performance; phase-advance for reducing the roll-off rates at crossover; and phase-lag to increase the roll-off rates at high frequencies should all be placed in W_p if desired.
   - W_a is a constant that aligns the singular values at a desired bandwidth (optional). This is effectively a constant decoupler and should not be used if the plant is ill-conditioned in terms of large RGA elements.
   - W_g is an additional gain matrix to provide control over actuator usage (optional). It is diagonal and adjusted so that the actuator rate limits are not exceeded for reference demands and typical disturbances on the scaled plant outputs.

For multimodel controller design, we have two options in choosing the compensators:

1) Choose a fixed set of pre- and/or post-compensators for all operating points.
2) Choose different sets of pre- and/or post-compensators at different operating points.

Obviously, the first method is simple. However, due to different gains of the models at different operating points, the resulting open-loop shapes will certainly be different, that means at different operating points the performance specifications are different, which is undesired. The most desired is that at all the operating points, we specify the same open-loop shapes. However, it is not always possible due to system nonlinearity. Note that in process control most of the disturbance arises at the low frequency, so we will choose sets of compensators such that the desired open-loop shapes at all operating points are almost the same at the low frequency, which means that the closed-loop systems will have similar disturbance rejection ability at all operating points.

Once local controllers are designed, we can form the global controller by switching, or using weights (fuzzy logic). We will use membership functions to create a transition region according to the operating point z,

$$u(t) = \sum_{i=1}^{k} u_i(t)\rho_i(z) \tag{15}$$

where k is the number of operating points, $u_i(t)$ is the output of the ith local controller, and $\rho_i(z)$ is the membership function of the ith local controller. There are many membership functions available. We will use trapezoidal functions in the examples below.

V. Illustrative Examples

Two examples will be used to illustrate the proposed method.

Example 1: Isothermal CSTR: Consider an isothermal continuous-flow stirred-tank chemical reactor (CSTR) in which a first-order irreversible reaction takes place [13], [14]. The relevant mass balance is

$$\frac{dC_A}{dt} = -kC_A + (C_{Ai} - C_A)u \tag{16}$$

where C_A is the reactant concentration, $u = q/V$ is the input, and C_{Ai} is the feed concentration. Reactor volume V is 2000 l, C_{Ai} is 1.0 mol l^{-1}, reaction temperature is 350K and the rate constant k is 0.028 min^{-1}.

The steady-state input-output map of the system is shown in Fig. 2.

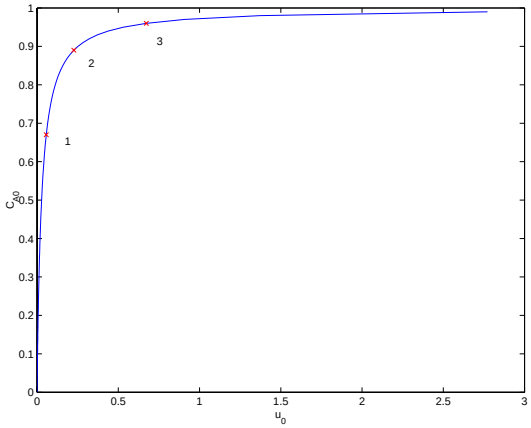

Fig. 2. Steady-state map: Example 1

For a prescribed 'distance' level $\gamma = 0.5$, starting from $C_{A0} = 0$, along the steady states, it can be shown that three operating points are needed to cover the entire range of C_{A0}. The three operating points correspond to

$$\begin{aligned} &1.\quad C_{A0} = 0.66;\\ &2.\quad C_{A0} = 0.83;\\ &3.\quad C_{A0} = 0.91. \end{aligned} \tag{17}$$

It is clear that the nonlinearity of the system lies at large values of C_{A0}. We then need three operating points to design

multimodel controllers, with each local controller will have a robustness margin of at least 0.5 at each operating point.

To include other performance specifications, e.g., rejection of steplike disturbances and attenuation of measurement noise, we specify the desired open-loop shape as follows:

- Magnitude is at least 40dB at low frequency range (from 0 to 10^{-2} rad/s);
- Magnitude is at most -20dB at high frequency range (from 10^2 to ∞ rad/s);
- Roll-off rate is at most -20dB/dec at medium frequency range.

With this specification, a pre-compensator W_1 can be chosen as

$$W_1 = K(1+\frac{1}{s}) \tag{18}$$

where the gain K is adjusted at different operating points. The post-compensator is chosen as $W_2 = 1$. Now with the same prescribed 'distance' level $\gamma = 0.5$, starting from $C_{A0} = 0$, along the steady states, we find that we also need three operating points to cover the entire range of C_{A0}. The three operating points correspond to

$$\begin{array}{ll} 1. & C_{A0} = 0.67; W_1 = 0.598(1+1/s); \\ 2. & C_{A0} = 0.89; W_1 = 5.289(1+1/s); \\ 3. & C_{A0} = 0.96; W_1 = 40(1+1/s). \end{array} \tag{19}$$

The three operating points are labeled with 'x' in the steady-state map (Fig. 2).

The sigma plots of the shaped open-loop plants at the operating points given above are shown in Fig. 3. They are almost equal at low frequencies, which guarantees that at each operating point the local controller will have similar disturbance rejection ability.

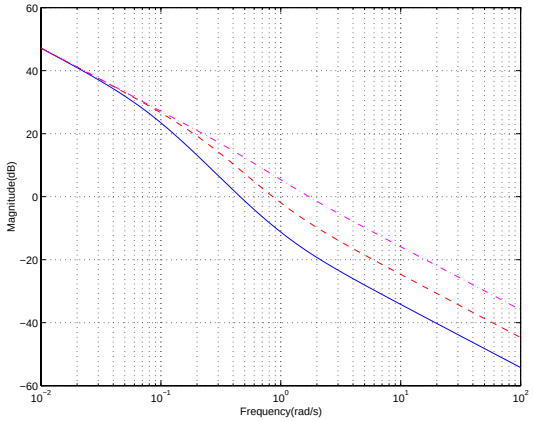

Fig. 3. Desired open-loop shapes: Example 1 (solid: operating point 1; dashed: operating point 2; dashdotted: operating point 3)

The gap metrics between the shaped plants at the three operating points and $\tilde{P}_0$ (corresponding to $C_{A0} = 0$) and $\tilde{P}_4$ (corresponding to $C_{A0} = 0.99$) are shown in Table I. The robustness margins computed by Eq.(10) at three operating points are shown in the last column of the table. Because

TABLE I

GAP METRICS BETWEEN SHAPED PLANTS: EXAMPLE 1

δ	$\tilde{P}_0$	$\tilde{P}_1$	$\tilde{P}_2$	$\tilde{P}_3$	$\tilde{P}_4$	b_{opt}
$\tilde{P}_0$	0	0.500	0.789	0.901	0.946	–
$\tilde{P}_1$	0.500	0	0.489	0.754	0.890	0.518
$\tilde{P}_2$	0.789	0.489	0	0.442	0.775	0.596
$\tilde{P}_3$	0.901	0.754	0.442	0	0.553	0.679
$\tilde{P}_4$	0.946	0.890	0.775	0.553	0	–

the linearized model is singular at $C_{A0} = 1$, we choose $C_{A0} = 0.99$ as the end point. The gap metric between P_3 and P_4 is greater than 0.5, however, since the robustness margin is also greater than 0.553, and the values of C_A at two operating points are close, we do not need more operating points within the small range of C_A from 0.96 to 1.

The three local controllers can be computed from Eq.(10).

$$K_1 = \frac{0.970s^2 + 1.198s + 0.229}{s^2 + 0.642s}, \tag{20}$$

$$K_2 = \frac{7.123s^2 + 10.384s + 3.261}{s^2 + 0.830s}, \tag{21}$$

$$K_3 = \frac{43.21s^2 + 78.91s + 35.703}{s^2 + 0.964s}. \tag{22}$$

To obtain a global controller, we use the membership functions shown in Fig. 4 for the three local controllers.

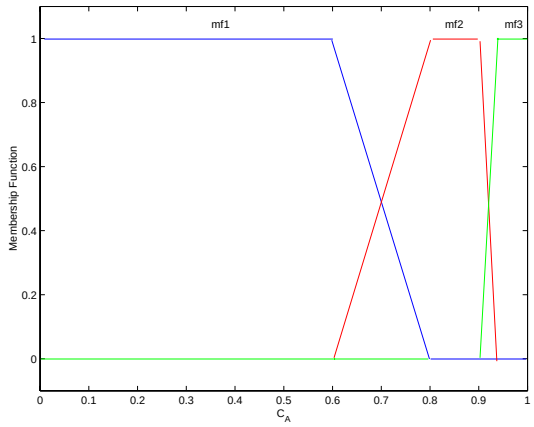

Fig. 4. Membership functions of local controllers

Simulations are done for the global controller with setpoints changing in the whole range of the operating points. One simulation result is shown in Fig. 5. It can be shown that the global controller will have large overshoot for setpoint step change (dash line in Fig. 5). It is not surprising since when we design local controllers we aim at achieving good disturbance rejection. The problem can be simply overcomed by adding a setpoint filter. In this example, the filter is chosen as $\frac{1}{4s+1}$ which gives good setpoint tracking as shown with the solid line in Fig. 5.

Example 2. Nonisothermal CSTR: The gap metric for the shaped plants gives similar operating points as those

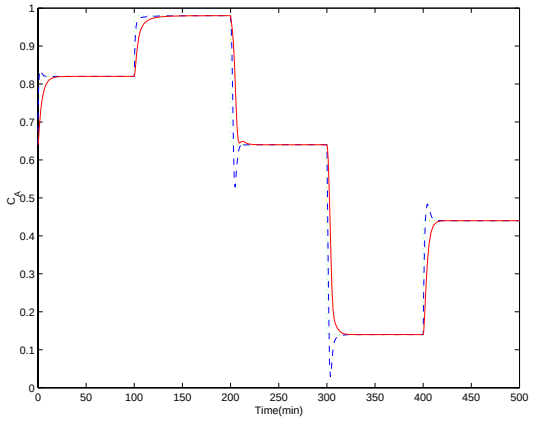

Fig. 5. Closed-loop responses of the CSTR: Example 1 (solid: with filter; dashed: without filter; dashdotted: setpoint)

predicted by the gap metric for the original models in the previous example. However, this is not always the case, as will be shown in this example.

Consider a nonisothermal CSTR where an irreversible, first-order reaction takes place [15]. The mathematical model is

$$\begin{cases} \dot{x}_1 &= -x_1 + D_a(1-x_1)\exp(-\frac{x_2}{1+x_2/\gamma}) \\ \dot{x}_2 &= -x_2 + BD_a(1-x_1)\exp(-\frac{x_2}{1+x_2/\gamma}) + \beta(u-x_2) \\ y &= x_2 \end{cases} \tag{23}$$

where x_1, x_2, and u are the dimensionless reagent conversion, the temperature, and the coolant temperature, respectively. The nominal values for the constants are $D_a = 0.072$, $\gamma = 20$, $B = 8$, and $\beta = 0.3$. The system is interesting in that it exhibits output multiplicity. Further, linearized systems at some equilibrium points are stable, and at some others, unstable.

The steady-state map of the system is shown in Fig. 6.

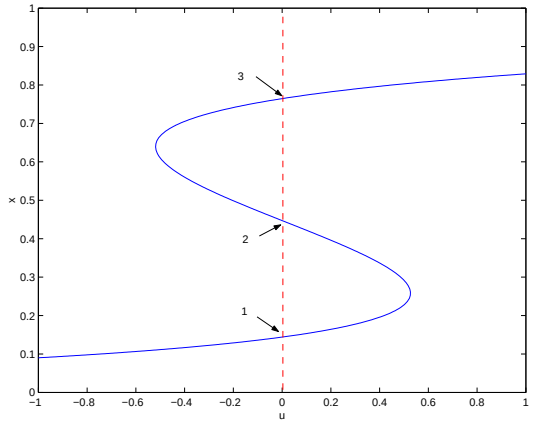

Fig. 6. Steady state map: Example 2

Three typical operating points are usually considered in multimodel controller design [4].

$$\begin{array}{ll} 1. & u_0 = 0, x_{10} = 0.144, x_{20} = 0.886, G_1 = \frac{0.3s+0.35}{s^2+1.41s+0.46}; \\ 2. & u_0 = 0, x_{10} = 0.447, x_{20} = 0.75, G_2 = \frac{0.3s+0.53}{s^2+0.36s-0.41}; \\ 3. & u_0 = 0, x_{10} = 0.765, x_{20} = 4.70, G_3 = \frac{0.3s+1.29}{s^2+1.6s+1.6}. \end{array} \tag{24}$$

So the local model at operating point 2 is unstable, while the models at operating points 1 and 3 are stable. The gap metric between G_2 and G_1 (G_3) is 1, which indicates that operating point 2 is quite far away from operating points 1 and 3. However, with performance weights, the shaped models at the three operating points are not so far.

For instance, choose the post-compensator $W_2 = 1$ and the pre-compensator $W_1 = K(6+3/s)$, where K is adjusted at different operating points to have almost the same magnitude at low frequency. For the three operating points, we have

$$\begin{array}{ll} 1. & W_1 = 1.6(6+3/s); \\ 2. & W_1 = 6+3/s; \\ 3. & W_1 = 1.6(6+3/s). \end{array} \tag{25}$$

The sigma plots of the shaped open-loop systems at the operating points given above are shown in Fig. 7.

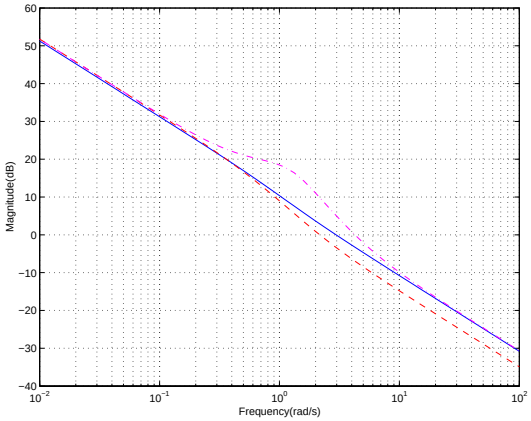

Fig. 7. Desired open-loop shapes: Example 2 (dashed: operating point 1; solid: operating point 2; dashdotted: operating point 3)

TABLE II

GAP METRICS BETWEEN SHAPED PLANTS: EXAMPLE 2

δ	$\tilde{P}_1$	$\tilde{P}_2$	$\tilde{P}_3$	b_{opt}
$\tilde{P}_1$	0	0.371	0.352	0.690
$\tilde{P}_2$	0.371	0	0.470	0.536
$\tilde{P}_3$	0.352	0.470	0	0.619

The gap metrics between the shaped plants at the three operating points are shown in Table II. The robustness margins computed by Eq.(10) at three operating points are shown in the last column of the table. Clearly the distances between the shaped models are small compared with the robustness margin at each operating point. Further computation shows that the distance between the shaped model at any of the operating point above and any shaped

model along the steady states is less than 0.5, which means that we need only one operating point to achieve the desired performance at the entire operating range.

The three local controllers can be computed from Eq.(10).

$$K_1 = \frac{10.067s^3 + 20.519s^2 + 12.994s + 2.626}{s^3 + 1.647s^2 + 0.574s}, \quad (26)$$

$$K_2 = \frac{9.453s^3 + 17.082s^2 + 9.287s + 1.554}{s^3 + 2.133s^2 + 0.816s}, \quad (27)$$

$$K_3 = \frac{12.212s^3 + 34.797s^2 + 23.384s + 4.942}{s^3 + 3.682s^2 + 1.115s}. \quad (28)$$

With a setpoint filter $\frac{1}{s+1}$, the responses of the closed-loop systems for the three controllers are shown in Fig. 8. All controllers give good setpoint tracking at the entire operating range.

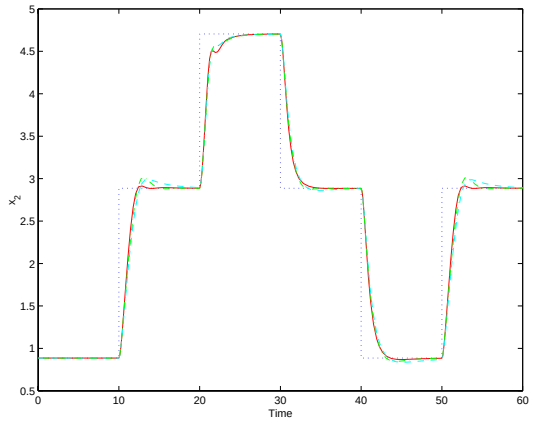

Fig. 8. Closed-loop responses of the CSTR: Example 2 (dashed: K_1; solid: K_2; dashdotted: K_3; dotted: setpoint)

Sometimes a nonlinear model is not the same as the real process, then there will be uncertainties in the local models. Since the local controllers are designed with the robustness in mind, the global controller is expected to be able to tolerate some uncertainties in the nonlinear model. It can be shown that the three controllers all work well when there are uncertainties in the model parameters D_a, B, β and γ. Fig. 9 illustrates the responses of K_1 for the case that the parameter β is increased or decreased by 30%.

VI. Conclusions

The method of using the gap metric for selecting operating points in multimodel controller design was extended to accommodate the performance requirement. With the loop-shaping $\mathcal{H}_\infty$ approach, the procedure of selecting operating points and the local controller design can be integrated. The local controllers can guarantee not only stability but also performance specified by the pre- and/or post-compensators. Thus at each operating points, local controllers can have similar performance, and the global performance of the system can be predicted.

Though the performance weighted gap metric is shown to be very useful in multimodel controller design, a drawback

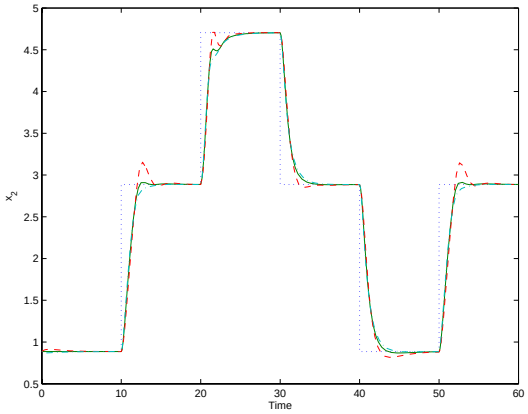

Fig. 9. Closed-loop responses of the CSTR: Parameter uncertainty (solid: nominal β; dashed: β increased by 30%; dashdotted: β decreased by 30%)

is that the distance of the local models is dependent on the compensators, which make it somehow difficult to determine the operating points without advance knowledge of the achievable closed-loop performance. Further research thus should be done to have a better measure of distance between systems, with performance in mind.

References

[1] R. Murray-Smith and T. A. Johansen, *Multiple Model Approaches to Modeling and Control*. London: Taylor & Francis, 1997.

[2] O. Galan, A. Palazoglu, and J. A. Romagnoli, "Robust H_∞ control for nonlinear plants based on multi linear models – an application to a bench scale pH neutralization reactor," *Chem. Eng. Sci.*, vol. 55, p. 4435, 2000.

[3] J. A. Rodriguez, J. A. Romagnoli, and G. C. Goodwin, "Supervisory multiple regime control," *Journal of Process Control*, vol. 13, pp. 177–191, 2003.

[4] O. Galan, J. A. Romagnoli, A. Palazoglu, and Y. Arkun, "Gap metric concept and implications for multilinear model-based controller design," *Ind. Eng. Chem. Res.*, vol. 42, pp. 2189–2197, 2003.

[5] K. H. McNichols and M. S. Fadali, "Selecting operating points for discrete-time gain scheduling," *Computers and Electrical Engineering*, vol. 29, pp. 289–301, 2003.

[6] M. Guay, "Measurement of nonlinearity in chemical process control," Ph.D. dissertation, Queen's University at Kingston, Ontario, 1996.

[7] A. Helbig, W. Marquardt, and F. Allgower, "Nonlinearity measures: Definition, computation and applications," *Journal of Process Control*, vol. 10, pp. 113–123, 2000.

[8] D. C. McFarlane and K. Glover, *Robust Controller Design Using Normalized Coprime Factorization Description*. Springer-Verlag, 1990.

[9] A. El-Sakkary, "The gap metric: robustness of stabilization of feedback systems," *IEEE Trans. Automat. Contr.*, vol. 30, pp. 240–247, 1985.

[10] T. Georgiou and M. Smith, "Optimal robustness in the gap metric," *IEEE Trans. Automat. Contr.*, vol. 35, pp. 673–686, 1990.

[11] K. Zhou and J. C. Doyle, *Essentials of Robust Control*. Prentice Hall, 1998.

[12] S. Skogestad and I. Postlethwaite, *Multivariable Feedback Control: Analysis and Design*. Wiley, 1996.

[13] M. A. Henson and D. E. Seborg, "Input-output linearization of general nonlinear processes," *AIChE Journal*, vol. 36, no. 11, pp. 1753–1757, 1990.

[14] F. J. Doyle, H. S. Kwatra, and J. S. Schwaber, "Dynamic gain scheduled process control," *Chem. Eng. Sci.*, vol. 53, no. 15, pp. 2675–2690, 1998.

[15] A. Uppal, W. H. Ray, and A. B. Poore, "On the dynamic behavior of continuous stirred tanks," *Chem. Eng. Sci.*, vol. 29, pp. 967–985, 1974.